Modeling of Steel-Concrete Composite Elements under In-Plane and Out-of-Plane Loads

Trevor D. Hrynyk[1] and Frank J. Vecchio, M.ASCE[2]

Abstract: A nonlinear analysis procedure for steel-concrete (SC) composite structures is presented. The procedure uses smeared crack concrete constitutive modeling done on the basis of the disturbed stress field model and supplemental material models that are used to incorporate response contributions of the steel faceplates comprising SC composite elements. The procedure is implemented within the framework of a thick-shell finite-element analysis program and is verified using experimental data pertaining to SC composite structural elements subjected to exclusively in-plane or exclusively out-of-plane (i.e., through-thickness) loading conditions. Lastly, the shell structure analysis program is used to numerically investigate the performance of SC composite elements subjected to combined in-plane and out-of-plane shear forces, an area directly relevant to SC infrastructure applications, yet one that is limited in the existing database of literature. **DOI:** [10.1061/(ASCE)ST.1943-541X.0001554](https://doi.org/10.1061/(ASCE)ST.1943-541X.0001554). © 2016 American Society of Civil Engineers.

Author keywords: Steel-concrete (SC) composite; Steel-concrete composite; Shells; Out-of-plane shear; Nonlinear analysis; Finite element; Analysis and computation.

Introduction

Steel-concrete (SC) composite wall sections are large structural elements comprised of thick concrete core sections and reinforced with comparatively thin steel faceplates. The concrete comprising these sandwich-type elements typically does not contain conventional in-plane or out-of-plane reinforcement. However, in addition to regularly spaced steel shear studs, through-thickness tie bars are used to anchor the faceplates to the concrete and to function as out-of-plane shear reinforcement. An illustration of the modular SC composite element is presented in Fig. 1.

The nuclear power industry had been the primary driving force in the initial design, development, and implementation of SC composite systems. However, the feasibility of using SC construction in applications outside of nuclear structures continues to be examined. Examples of SC construction applications that have been investigated include offshore structures designed to resist extreme loads due to high intensity waves or iceberg impacts (Link and Elwi 1995), tunnel liners and wall assemblies (Tanaka et al. 1998), and modular framed building systems (Takeuchi et al. 1998). It is likely that efforts focused toward identifying other potential applications for SC composites will continue as the prefabricated natures of these systems are attractive and in line with demands for accelerated and modular construction practices.

A significant amount of experimental work has been undertaken to evaluate the performance of SC composite elements under different in-plane and out-of-plane loading scenarios. Studies include SC wall assemblies subjected to axial compression testing (Usami et al. 1995), SC panel-type elements loaded under in-plane shear stress (Ozaki et al. 2004), SC shear wall assemblies under varied combinations of axial load and shear (Sasaki et al. 1995; Takeuchi et al. 1998; Epackachi et al. 2014), and SC beam-type elements subjected to out-of-plane (through-thickness) shear loading conditions (Link and Elwi 1995; Malushte et al. 2009; Sener and Varma 2014). In the large majority of these studies, the experimental results have shown that SC composite elements are generally capable of achieving strengths that are similar or, in many cases, greater than those obtained by conventional RC elements of comparable construction. However, in several investigations, reported damage mechanisms that are unique to SC construction ultimately governed element capacity and were deemed responsible for degradation of element stiffness.

SC Composite Analysis Procedures

In comparison to the significant volume of experimental research that has been carried out to investigate the performance of SC composite wall elements, research dedicated toward the development of reliable SC modeling procedures is limited. Much of the existing analytical and computational procedures used to investigate SC structure response consider one of two approaches: (1) strut-and-tie or truss model idealizations that have met with some success for member-level design and assessment applications; and (2) finite-element procedures that have been used in system level assessment and design of SC infrastructure. In the case of finite-element procedures, the typical approach used for SC structures has been to utilize powerful general purpose finite-element software packages and apply them in a micromodeling fashion. These procedures require extremely fine meshing techniques typically involving dense distributions of three-dimensional solid finite elements. Examples of these modeling techniques used for the analysis of SC composite infrastructure are presented by Varma et al. (2011) and Epackachi et al. (2014). Although such procedures are capable of providing highly detailed representations of SC composite structures, they are computationally expensive, and most of the available commercial software programs that are used for such simulations utilize concrete constitutive formulations that

[1]Assistant Professor, Dept. of Civil, Architectural and Environmental Engineering, Univ. of Texas at Austin, Austin, TX 78712 (corresponding author). E-mail: thrynyk@utexas.edu

[2]Professor, Dept. of Civil Engineering, Univ. of Toronto, Toronto, ON, Canada M5S 1A4.
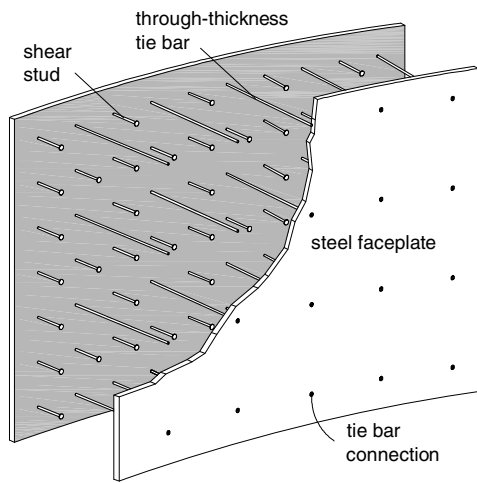
Fig. 1. SC composite wall element concept

have been developed on the basis of small-scale unreinforced and, in many cases, uncracked concrete elements. Thus, the suitability of their generalized application for the assessment of large-scale cracked SC composite structures is generally unfounded.

In recent years, alternative analytical approaches utilizing smeared crack modeling procedures and concrete constitutive relations formulated specifically for cracked RC have been used in the analysis of SC elements and subassemblies (Zhou et al. 2010; Vecchio and McQuade 2011). In many regards, such approaches can be viewed as more practical modeling procedures for the analysis of SC infrastructure because their smeared treatment of cracked concrete typically permits simple finite-element model creation and reduced computation cost, but still allows for explicit implementation of many of the unique and influential behavioral mechanisms that are known to occur as a result of the interactions between steel reinforcement and cracked concrete.

In the procedure presented by Vecchio and McQuade (2011), a single-plane stress element was formulated to represent the integral response of both the concrete and the steel faceplates comprising the SC composite. Cracked concrete material modeling was done on the basis of the formulations of the disturbed stress field model (DSFM) (Vecchio 2000), a hybrid rotating-fixed smeared crack model developed by way of extending the formulations of the modified compression field theory (MCFT) (Vecchio and Collins 1986). The material response of the faceplates was modeled according to a trilinear elastic-plastic strain hardening constitutive model combined with the von Mises yield criterion to account for the influence of biaxial stress conditions. Using a set of default material models and basic finite-element modeling procedures (i.e., no link or contact elements, simple meshing procedures, predefined material models), the SC element analysis procedure was shown to provide good agreement with experimental data and produced reliable estimates of SC member strengths and failure modes.

This paper presents work done to expand the two-dimensional DSFM-based SC element formulations developed previously by Vecchio and McQuade (2011) for the application of three-dimensional SC composite shell structure modeling. Modeling assumptions similar to those made by Vecchio and McQuade (2011) regarding steel faceplate-concrete interaction behavior are used, however, within the framework of a layered thick-shell finite-element program and with some modifications of the material modeling procedures. Verification studies used to assess the adequacy of the SC shell element analysis procedure in capturing the

response of different types of SC elements involving in-plane and out-of-plane loading conditions are presented. The resulting procedure is used to numerically investigate the response of an SC composite wall element under combined in-plane and out-of-plane shear forces, an area directly relevant to the application of SC composite shell structures, yet one that is currently absent from the database of SC-related literature.

Proposed SC Modeling Approach

Background of the Layered Thick-Shell Element

The SC composite analysis procedure presented in this work is implemented within the framework of a nonlinear analysis program using layered thick-shell finite elements. The program was originally developed by Figueiras and Owen (1984) for the analysis of conventional RC shells and slabs and, in its original state, had many noteworthy features. Perhaps of greatest significance, the shell structure analysis program accounted for the development of through-thickness shear deformations using Mindlin theory (Mindlin 1951) and employed a nine-noded quadratic heterosis shell element that was shown to provide good performance in both thick-shell and thin-shell applications. Subsequently implemented RC-dedicated nonlinear material modeling done in accordance with the formulations of the MCFT was shown to provide reasonable structural response estimates for a broad range of conventional RC slab and shell structures under in-plane and out-of-plane loading scenarios (Polak and Vecchio 1993). More recent procedural modifications done by Hrynyk and Vecchio (2015a) involved modifying the sectional analysis procedure used to incorporate out-of-plane shearing effects in the layered element formulation and implementing cracked concrete material modeling in accordance with the formulations of the DSFM (Vecchio 2000). With the implementation of the noted modifications, the RC shell structure analysis procedure has been shown to accurately capture out-of-plane shear failures in RC slabs and shells subjected to complex loading conditions, including loading scenarios involving combined in-plane and out-of-plane shear forces. The work presented in Hrynyk and Vecchio (2015a) serves as the framework used for the development of the SC composite shell element modeling procedure presented in this paper and provides additional details regarding the material modeling procedures that had been used for conventional RC structures.

In its current state, the through-thickness response of the layered thick-shell element is based on the assumptions that, in accordance with Mindlin theory, (1) plane sections remain plane, but not necessarily normal to the element midsurface; and (2) out-of-plane normal stresses (i.e., stresses in the local z-direction) are negligible. According to the through-thickness layered shell formulation presented by Hrynyk and Vecchio (2015a), it is also assumed that (3) the effective out-of-plane shear strain distribution used to calculate cracked concrete material behavior, which is analogous to a net concrete strain distribution, can be approximated as being parabolic through the thickness of the shell element. The layered shell element and the assumed through-thickness strain variations noted in Assumptions 1 and 3 are illustrated in Fig. 2.

Constitutive Modeling

In the SC composite shell element analysis procedure, concrete and steel faceplate material layers are analyzed individually and provide unique contributions toward the shell finite-element stiffness matrix. Steel faceplates are uniquely defined for each planar surface of the shell element and, as such, the faceplates need not be the
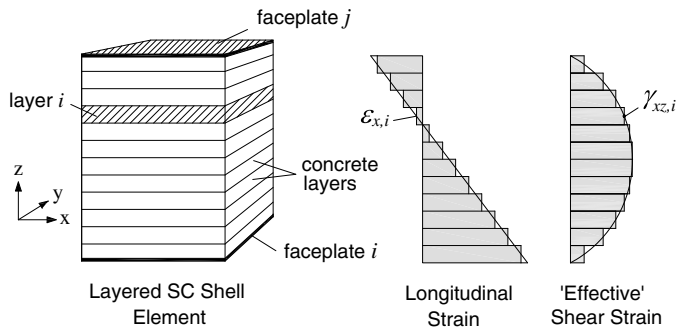
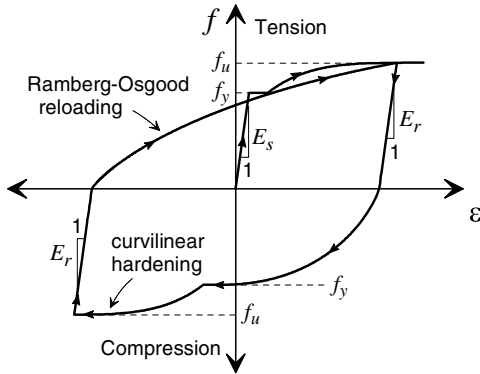**Fig. 2.** Layered shell element through-thickness strain variation

Fig. 3. General hysteretic response for Seckin (1981) model with nonlinear hardening

same thickness nor have the same material properties. Out-of-plane reinforcement attributed to through-thickness tie bars are also explicitly analyzed but are treated as a smeared property of the core concrete layers.

Cracked concrete material modeling is done on the basis of the formulations of the DSFM (Vecchio 2000), a generalized approach for modeling the behavior of RC elements subjected to biaxial loading conditions. This smeared crack analysis procedure, developed specifically for cracked reinforced concrete elements, inherently considers the redistribution of internal forces resulting from stiffness changes arising from cracking or crushing of concrete, average postcracking concrete tensile stresses stemming from the interaction between bonded steel reinforcing bars and concrete, concrete compression softening resulting from the presence of coexisting lateral tensile strains and compressive stresses acting on cracked reinforced concrete elements, and the effects of variable and changing crack widths (including slip deformations along crack surfaces). Additional details regarding the application of the DSFM within the framework of the three-dimensional shell element modeling procedure considered are provided elsewhere (Hrynyk and Vecchio 2015a).

Constitutive modeling of the steel faceplates was done according to the formulation presented by Seckin (1981) with the subsequent procedural modifications presented in Wong et al. (2013). The modeled faceplate stress-strain response consists of an initial linear-elastic phase followed by a yield plateau and nonlinear strain hardening phase and incorporates the Bauschinger effect in the material hysteresis (Fig. 3). The von Mises yielding criterion [Eq. (1)] was used to estimate the yield strength of the steel faceplates under biaxial stress states. Because parabolic out-of-plane shear strain distribution is considered for the layered shell
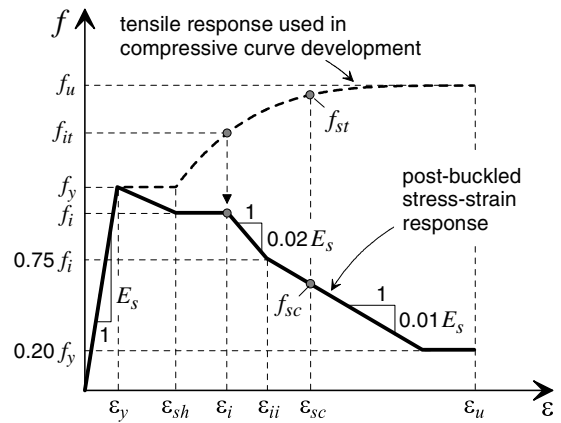

Fig. 4. Steel faceplate postbuckling compressive response

element, out-of-plane shear strain development in the thin steel faceplates is assumed to be negligible (Fig. 2). Thus, the modeled response of the faceplates only considers in-plane stress conditions

$$(f_{sp1} - f_{sp2})^2 + (f_{sp2} - f_{sp3})^2 + (f_{sp3} - f_{sp1})^2 = 2(f_y)^2 \qquad (1)$$

where f_{sp1}, f_{sp2}, and f_{sp3} represent the principal stresses acting on the steel faceplate; and f_y represents the uniaxial yield strength of the faceplate steel. However, with the assumptions that out-of-plane shear and out-of-plane normal stress development in the steel faceplates are negligible, one of the three principal stresses acting on the faceplates will always be equal to zero in this formulation.

Two models have been used to incorporate steel faceplate buckling: (1) the modified Euler elastic buckling expression presented by Usami et al. (1995) [Eq. (2)]; and (2) a refinement of the postbuckling stress degradation model originally presented by Dhakal and Maekawa (2002a, b) for conventional steel reinforcing bars. In the model presented by Usami et al. (1995), the critical elastic buckling stress, σ_{cr}, of stud-anchored steel faceplates with stud spacing to plate thickness ratios of b/t is approximated by using

$$\sigma_{cr} = \pi^2 E_s / [12\eta^2(b/t)^2] \qquad (2)$$

where $\eta = 0.7$; and E_s = modulus of elasticity of the steel faceplates.

A refined version of the model developed by Dhakal and Maekawa (2002a, b) is used to supplement the Usami et al. (1995) elastic plate buckling model presented in Eq. (2) by providing an estimate of the postbuckled stress-strain responses for the steel faceplates. Once plate buckling is estimated to occur, the postbuckled compressive stress, f_{sc}, is computed on the basis of the faceplate compressive strain, ε_{sc}, the fictitious tensile faceplate stress, f_{st}, associated with the magnitude of the compressive strain, and the b/t ratio of the faceplate. The generalized postbuckled compression stress-strain response developed from the refined Dhakal-Maekawa relationship is presented in Fig. 4. Related formulas and additional details necessary for the usage of the refined Dhakal-Maekawa model are presented in Wong et al. (2013). For the purpose of modeling the plate buckling response in SC composite elements, the stud spacing to plate thickness ratio, b/t, is used in place of the conventional rebar length to diameter ratio that serves as a main parameter in the Dhakal-Maekawa model and the subsequent model refinement.
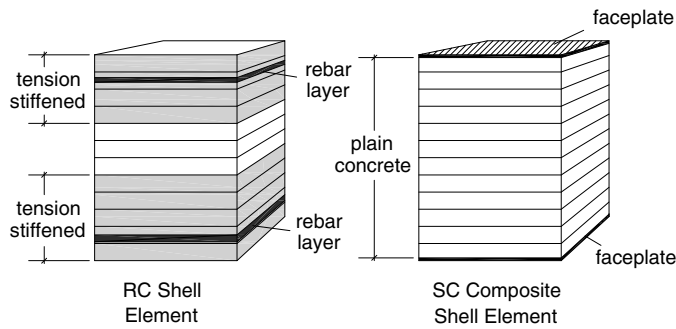
Fig. 5. Treatment of tension stiffening effects

Assumptions

Similar to the DSFM-based smeared crack modeling approach used by Vecchio and McQuade (2011), three key assumptions have been made regarding the modeling of the steel faceplate–concrete core interaction. Specifically, the following are assumed:

1. Steel faceplate contributions toward concrete tension stiffening are negligible: In the modeling of conventional RC shell elements, the influence of tension stiffening effects are considered in concrete regions located within a tributary distance of 7.5 times the diameter of any deformed steel reinforcing bar (Fig. 5), as recommended by CEB-FIP MC 1990 (CEB-FIP 1993). Because tension stiffening is known to be attributed to bond-related mechanisms developed between deformed reinforcing bars and surrounding concrete, it is unknown to what degree, if any, tension stiffening effects will be developed by way of smooth steel faceplates that are anchored to concrete using discretely spaced shear stud connectors. Moreover, relative to the thicknesses of the faceplates, the sectional geometries of the concrete cores comprising SC construction applications are large. Thus, even if bond-related tensile stresses are developed, conventional methods of evaluating effective tension stiffened regions would suggest that the majority of the concrete core would remain unaffected.

2. The average crack spacing of SC composite elements is equal to the total element thickness: Several crack spacing models have been proposed for conventional RC elements reinforced with deformed and/or smooth steel reinforcing bars. In the DSFM, average crack spacings are computed on the basis of CEB-FIP MC 1990 (CEB-FIP 1993) and are used to evaluate average crack widths. The influences of variable and changing crack widths bear heavily on the local element response considered in the DSFM. Additionally, element crack spacings and crack widths also play a role in the computation of the post-cracking tensile stress degradation of unreinforced concrete element regions (i.e., the tension softening response), a significant consideration given that SC element tension stiffening effects are deemed negligible in the proposed procedure (Fig. 5).

   In modern RC design and modeling provisions, e.g., AASHTO (2014), FIB MC 2010 (FIB 2012), and CSA A23.3 (CSA 2004), the maximum crack spacing of one-way beam-type/frame-type members is limited to the distance between layers of crack-control reinforcement. Where none is provided other than the primary flexural reinforcement, the maximum crack spacing is set as the effective depth of the member. Thus, it is assumed that the maximum crack spacing for SC elements can be conservatively assumed as being approximately equal to the overall through-thickness depth of the element (center-to-center distance of the steel faceplates).

3. The shear stud connectors are not adequate in preventing interfacial slip: In the work of Zhang et al. (2014), it was shown that typical stud connector details provided for SC composite wall elements are generally not adequate to achieve fully composite behavior; however, it was noted that that the development of only partially composite action led to minimal reduction of the flexural stiffness of SC composite elements. A prior numerical investigation performed using the SC composite analysis procedure presented in this work (Hrynyk and Vecchio 2015b) found that the use of a perfect interfacial bond assumption led to significant lateral (i.e., confining) stress development in both the steel faceplates and the concrete core sections and ultimately led to overestimations of SC composite element capacity. Thus, to preempt the development of artificial lateral stresses attributed to the perfect faceplate-concrete core bond assumption inherent to the layered shell element formulation used, material lateral expansions (e.g., Poisson effects and concrete dilatation) have been neglected. Although this approach may only approximately incorporate the influences of interfacial slip, it negates the need for more complex modeling procedures (e.g., discrete stud representation, the use of link and contact elements) and is in keeping with the practical nature of the smeared crack composite element modeling procedure. This assumption differs from that used in the work done by Vecchio and McQuade (2011). Furthermore, neglecting material lateral expansions does influence the manner in which concrete confinement and dilatation are modeled in the cores of the SC elements. Although, in most cases, these mechanisms are likely of secondary relevance in comparison to the treatment of the interfacial slip, the development of passive lateral confinement can play a meaningful role on element response in certain situations. Examples of such cases are likely to occur in SC elements experiencing extensive concrete crushing leading to significant postcrushing concrete dilatation.

Material Matrix Development

The methodology used to develop the three-dimensional 6×6 material stiffness matrices for the concrete material layers, with or without through-thickness shear reinforcement and according to the formulations of the DSFM, is presented in Hrynyk and Vecchio (2015a). The material stiffness matrices for the steel faceplates comprising the SC composite shell elements are developed in a manner similar to that used for concrete material layers.

Assuming that the steel faceplates are perfectly bonded to the concrete core section of the SC element, the total strains developed in the ith steel faceplate are equal to the total strains in the concrete at the surface of the element. The set of total strains developed in the ith faceplate, ε_i, are comprised of (1) net strains, $\varepsilon_{sp,i}$; (2) elastic offsets, $\varepsilon_{sp,i}^o$; which could include thermal strains or lateral expansions attributable to the Poisson effect (if desired); and (3) plastic offsets, $\varepsilon_{sp,i}^p$, which are used to represent yielding and faceplate damage attributed to prior loading excursions

$$\{\varepsilon\}_i = \{\varepsilon_{sp}\}_i + \{\varepsilon_{sp}^o\}_i + \{\varepsilon_{sp}^p\}_i$$
$$= \langle\, \varepsilon_x \quad \varepsilon_y \quad \varepsilon_z \quad \gamma_{xy} \quad \gamma_{xz} \quad \gamma_{yz} \,\rangle_i \qquad (3)$$

Steel faceplate principal strains (ε_{sp1}, ε_{sp2}, ε_{sp3}) and their corresponding direction cosine vectors are calculated from the local net strain set presented in Eq. (3). Steel faceplate principal stresses ($f_{sp1}, f_{sp2}, f_{sp3}$) are computed on the basis of the steel faceplate constitutive models presented above. The secant moduli pertaining to the steel faceplate material stiffnesses in the principal stress directions are calculated as

$$\bar{E}_{sp1} = \frac{f_{sp1}}{\varepsilon_{sp1}}, \qquad \bar{E}_{sp2} = \frac{f_{sp2}}{\varepsilon_{sp2}}, \qquad \bar{E}_{sp3} = \frac{f_{sp3}}{\varepsilon_{sp3}} \qquad (4)$$

Secant shear moduli are calculated according to

$$\bar{G}_{sp12} = \frac{\bar{E}_{sp1} \cdot \bar{E}_{sp2}}{\bar{E}_{sp1} + \bar{E}_{sp2}}, \qquad \bar{G}_{sp13} = \frac{\bar{E}_{sp1} \cdot \bar{E}_{sp3}}{\bar{E}_{sp1} + \bar{E}_{sp3}},$$

$$\bar{G}_{sp23} = \frac{\bar{E}_{sp2} \cdot \bar{E}_{sp3}}{\bar{E}_{sp2} + \bar{E}_{sp3}} \qquad (5)$$

The 6×6 orthotropic steel faceplate material matrix, $[D_{sp}]'$, developed relative to the principal stress directions, is

$$[D_{sp}]' = \begin{bmatrix} \bar{E}_{sp1} & 0 & 0 & 0 & 0 & 0 \\ 0 & \bar{E}_{sp2} & 0 & 0 & 0 & 0 \\ 0 & 0 & \bar{E}_{sp3} & 0 & 0 & 0 \\ 0 & 0 & 0 & \bar{G}_{sp12} & 0 & 0 \\ 0 & 0 & 0 & 0 & \bar{G}_{sp13} & 0 \\ 0 & 0 & 0 & 0 & 0 & \bar{G}_{sp23} \end{bmatrix} \qquad (6)$$

Regardless of whether lateral expansions due to the Poisson effect are considered, the material stiffness matrix presented in Eq. (6) will always be diagonal. Additionally, because it is assumed that the steel faceplates are only subjected to in-plane stress conditions, one faceplate principal stress (f_{sp1}, f_{sp2}, f_{sp3}) will always equal zero. Hence, the faceplate material matrix presented in Eq. (6) will consist of three non-zero values: two secant moduli and one secant shear modulus.

Transformation from the principal axes to the local xyz coordinate system is performed with the use of an appropriate stiffness transformation matrix, $[T_{sp}]$ as described by Cook et al. (1989), giving the local steel faceplate material stiffness matrix, $[D_{sp}]$ as

$$[D_{sp}] = [T_{sp}]^T [D_{sp}]'[T_{sp}] \qquad (7)$$

The stresses in the steel faceplates are calculated using the following equilibrium relationship:

$$\{\sigma_{sp}\} = [D_{sp}]\{\varepsilon\} - \{\sigma_{sp}^o\} \qquad (8)$$

Because the net strain set is used in the development of the local steel faceplate material matrix, the pseudostress vector, $\{\sigma_{sp}^o\}$, is considered in the preceding equilibrium equation to incorporate the deformations associated with faceplate strain offsets [Eq. (3)]. Faceplate pseudostresses are calculated on the basis of Eq. (9)

$$\{\sigma_{sp}^o\} = [D_{sp}](\{\varepsilon_{sp}^o\} + \{\varepsilon_{sp}^p\}) \qquad (9)$$

Once computed, the local faceplate material matrix, $[D_{sp}]$, and the pseudostress matrix, $\{\sigma_{sp}^o\}$, are incorporated into the layered shell element secant stiffness matrix and the structure total load vector, respectively, using typical finite-element volume integration techniques (Cook et al. 1989). In a manner similar to that used for the concrete material layers (Hrynyk and Vecchio 2015a), the element stiffness and the applied load vector are continuously updated over the course of the analysis using an iterative solution procedure.

Verification

To assess the adequacy of the SC composite shell element analysis procedure, test data available in the open literature pertaining to SC

Table 1. Supplemental Material Models Used for Verification

Model description	Reference
Concrete compression curve	Hoshikuma et al. (1997)
Compression softening	Vecchio (2000)
Tension stiffening[a]	Bentz (2005)
Concrete confinement	Kupfer et al. (1969), Richart et al. (1928)
Crack slip distortions	Walraven and Reinhardt (1981)
Crack spacing[a]	CEB-FIP (1993)
Concrete hysteresis	Vecchio (2000)
Faceplate hysteresis	Seckin (1981)
Faceplate yield criteria	von Mises
Faceplate buckling	Usami et al. (1995), Wong et al. (2013)

[a]Attributed to tie bar reinforcement; faceplate contributions not considered.

members under in-plane and out-of-plane loading conditions have been used for verification. SC shear wall data are used to investigate the membrane performance of the SC composite analysis procedure, and data for SC beam-type elements are used to examine the performance of the layered thick-shell formulation for SC elements subjected to through-thickness shear. Details of the experimental studies considered are discussed and information regarding the finite-element modeling approach is provided. In addition to the constitutive formulations previously described, a common set of previously established default concrete material models were used to support the DSFM-based SC element analysis procedure. Finite-element meshing and layer discretization procedures established from previous studies were used as an aid in developing the finite-element models (Hrynyk 2013). A summary of the relevant material models used for the SC analyses reported in this work is provided in Table 1. Cases involving the use of alternative nondefault modeling parameters are clearly noted in the following discussions.

In-Plane Loading

Sasaki et al. (1995) reported the results from a series of flanged SC shear walls tested under cyclic in-plane loading conditions. The seven walls comprising the experimental program encompassed a broad range of variables: the ratio of bending moment to shear force, the steel plate reinforcement ratio, ρ_s, the level of axial compression, N, and the stud connector details comprising the web-flange intersection regions. Despite the variations in specimen details and testing conditions, the damage development reported for the SC walls was essentially common: following some initial cracking in the flanges and webs at the bases of the walls, the steel faceplates comprising these sections yielded and, thereafter, were noted to buckle. Posttest examination of the failed SC walls revealed that extensive concrete crushing occurred in the web regions forming the web-flange intersections of the walls, and several of the shear studs used to anchor the web plates to the concrete showed signs of bond failure or had fractured. Given the range of testing parameters considered, the Sasaki et al. (1995) testing program serves as a challenging data set for verification of SC analysis procedures.

The walls were constructed with heights ranging from 1,250 to 2,500 mm and web thicknesses ranging from 115 to 345 mm. All walls were constructed using 2.3-mm-thick steel faceplates in the web and flange regions, and the column regions of the walls were constructed using 4.5-mm-thick steel plates. Steel plates forming the web regions of the walls were anchored using steel studs spaced at 76 mm, resulting in a b/t ratio of 33. To increase the flexural capacities of the walls, bending stiffeners fastened to the edges of the flanges were provided (Fig. 6). The walls were constructed between thick RC boundary elements, which were used to restrain the bases of the walls, and transfer lateral loads. Because the SC
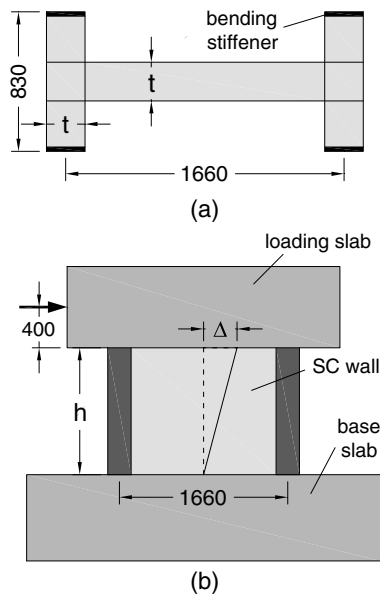
Fig. 6. Configuration of Sasaki et al. (1995) SC shear wall specimens: (a) cross section; (b) elevation

Fig. 7. Finite-element mesh for Sasaki et al. (1995) SC composite shear walls H10T10 and H10T10V

shell element analysis procedure used does not explicitly incorporate the influence of steel-concrete interfacial slip, one of the shear walls (H10T10N), which was constructed without steel studs at the web-flange intersection, was not analyzed. Cyclic displacements were applied to the loading slabs in the planar directions of the SC walls until a predefined level of wall deformation had been achieved. A summary of the geometries and reinforcement conditions for the six shear walls considered is presented in Table 2.

The SC shear walls were modeled using a combination of layered shell and truss bar finite elements (Fig. 7). Because the SC walls in the testing program were subjected to in-plane loading conditions only, the finite-element models of the walls were limited to planar translation by restraining all rotational and out-of-plane translational degrees of freedom associated with the shell elements. All SC shell elements consisted of three material layers: one concrete core layer and two layers representing the steel faceplates. For this idealized in-plane loading scenario, and considering that local tension stiffening effects attributed to the steel faceplates are neglected, no benefits would be attained by using a finer discretization of layers through the thickness of the SC shell elements. The faceplates comprising the flanges were modeled using truss bar elements. The bending stiffeners provided at the tips of the flanges were also modeled using truss elements to prevent the development of artificial confining effects at the web-flange intersection attributed to the two-dimensional modeling approach used. Details

Table 2. Sasaki Shear Wall Tests Used for In-Plane Verification

SC wall	Height, h (mm)	Thickness, t (mm)	Web reinforcement, ρ_s (%)
H07T10	1,250	230	2.00
H10T05	1,660	115	4.00
H10T10	1,660	230	2.00
H10T10V[a]	1,660	230	2.00
H10T15	1,660	345	1.33
H15T10	2,500	230	2.00

[a]Applied axial compressive stress of 3.0 MPa; axial load is zero for all other walls.
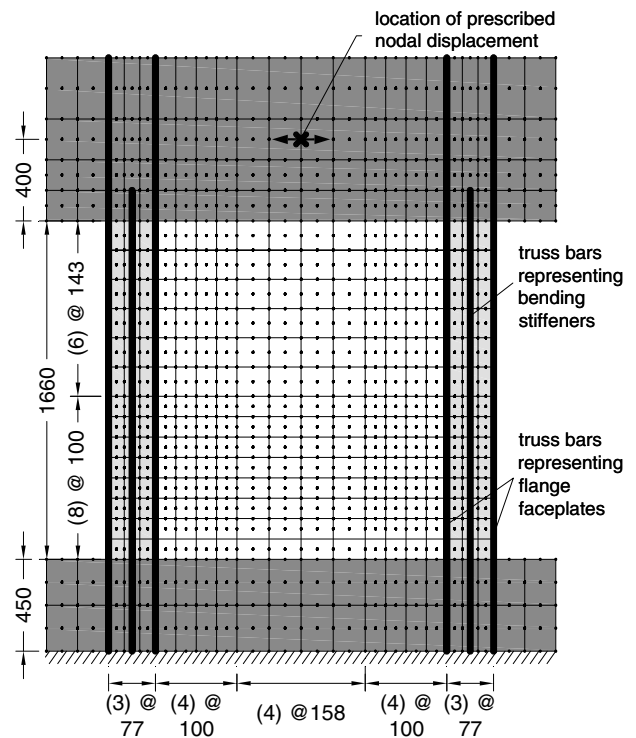
regarding the bending stiffeners were not provided in the original reference for the testing program; however, from the illustration of the test specimens provided by Sasaki et al. (1995), the bending stiffeners were estimated to be approximately 25 mm-thick with widths equal to the flange thicknesses, t. The base slabs were assumed to be 900 mm-deep; however, only half of the base slab height was included in the finite-element models. The bottom of the half-height base slab was restrained using a series of pinned nodal restraints.

The material properties used in the analyses were based on those reported (Sasaki et al. 1995). For all steel plates, strain hardening was assumed to initiate at a strain of 20×10^{-3} mm/mm, and the ultimate stress was assumed to occur at a strain of 180×10^{-3} mm/mm. A reversed cyclic displacement protocol was applied at a single nodal point located 400 mm above the top of the flanged section of the SC wall specimen. The loading protocol used in the testing program consisted of variable amplitude changes between load cycles, different numbers of load cycles at each displacement level, and included reduced amplitude excursions at several instances over the course of loading. However, to simplify the performance of the finite-element analyses, a cyclic loading protocol consisting of one reversed (i.e., one positive and one negative) displacement cycle at each amplitude level was considered. For the shortest wall (H07T10), a displacement step size of 0.375 mm was used to control the analysis, and the displacement cycling was performed using amplitude increments of 2.0 mm. For intermediate height walls (H10T05, H10T10, H10T10V, and H10T15), a displacement step size of 0.50 mm was used, and the displacement cycling was performed using increments of 2.0 mm. Lastly, for the tallest wall (H15T10), the analysis was performed using a displacement step size of 0.75 mm and a cyclic amplitude increment of 3.0 mm.

The computed shear force-displacement responses for the six SC shear walls are plotted alongside the experimental envelope
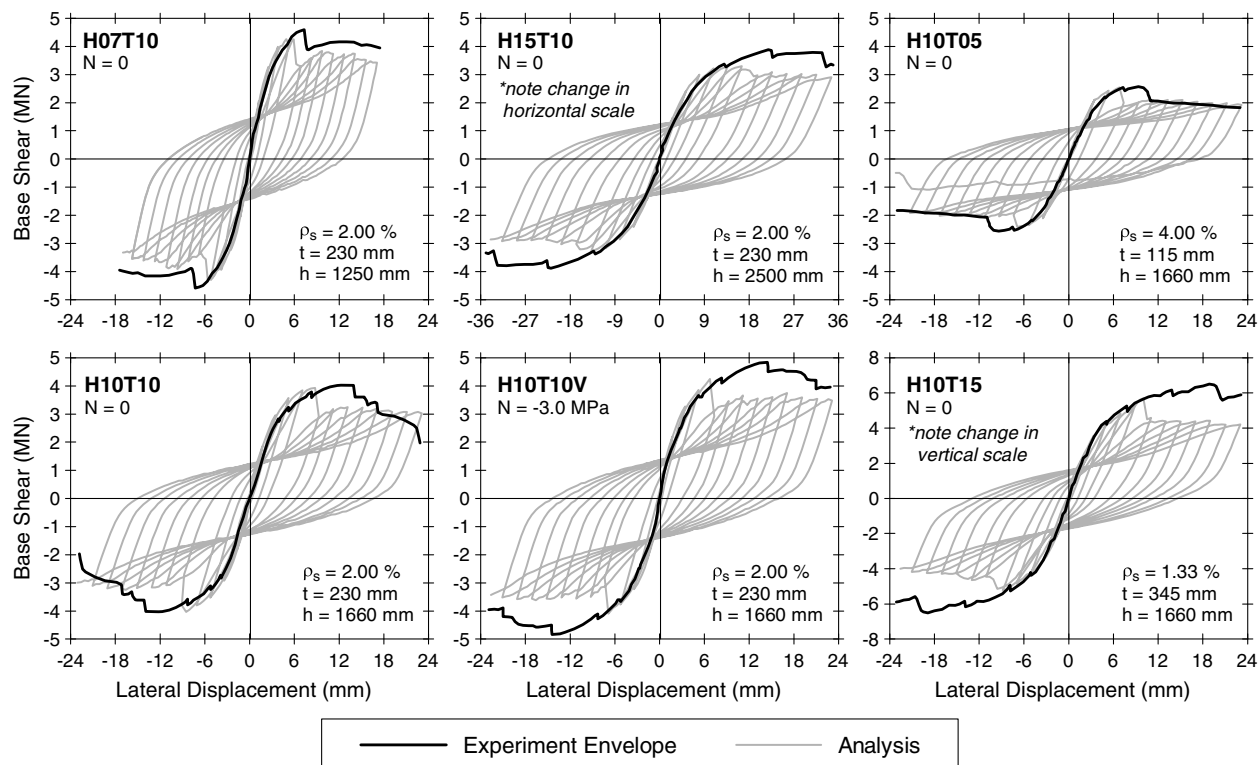
Fig. 8. Load-displacement results for Sasaki et al. (1995) SC composite shear walls

responses in Fig. 8. The analyses were shown successful in capturing the initial stiffnesses of the walls and, in most cases, provided reasonable estimates of wall capacity. The postpeak stiffness degradation of walls H07T10 and H10T05 were captured well; however, in the four other walls, the computed postpeak shear resistances were significantly lower than those measured in the experiments. In agreement with test observations, localized compressive deformations were estimated to develop at the bases of the wall webs, at locations corresponding to the web-flange intersections. Steel plate yielding followed by concrete crushing within these localized regions led to abrupt postpeak shear resistance reductions. In comparison to the experimentally measured responses, the computed onset of web plate buckling was estimated to occur prematurely and, in all cases, led to underestimates of wall capacity and ductility. This plate buckling was estimated to occur shortly after steel plate yielding and before the onset of web concrete crushing. In agreement with that reported from the experiments, very limited concrete crushing was estimated to develop in the flanges of the walls. Although some variation amongst the accuracies of the computational results obtained for the six SC walls is apparent from the load-displacement responses presented, the analysis procedure still provided a mean analytical-to-experimental strength ratio of 0.91 with a coefficient of variation of approximately 8%. Thus, considering the basic finite-element meshing procedures used and that no attempts were made to calibrate or refine the behavioral models or analysis parameters, the SC analysis procedure is considered to provide adequate response estimates for the shear walls comprising the Sasaki et al. (1995) test series.

Out-of-Plane Loading

In recent years, a great deal of research has focused on evaluating the behavior of SC wall elements under out-of-plane loading conditions. In the context of verifying the adequacy of the layered SC

shell element formulation, of particular interest is the work presented by Varma et al. (2011), which summarizes the details and findings of a testing program involving large-scale field-representative SC wall elements under out-of-plane shear forces. The four large-scale beam-like elements tested in the program were 914 mm deep, approximately 860 mm wide, and were tested under four-point monotonic loading conditions with clear spans that ranged from approximately 5.8 to 11.3 m. Three of the four large-scale beams (SP2-1, SP2-2, and SP2-3) contained through-thickness shear reinforcement provided by way of regularly spaced 19 mm-diameter tie bars that resulted in a uniformly distributed out-of-plane reinforcement ratio, ρ_v, of approximately 0.15%. The shear-reinforced SC beams were constructed with 19 mm-thick faceplates. Beam SP1-5, which did not contain any form of through-thickness shear reinforcement, was constructed with 13 mm-thick faceplates. Shear span-to-depth ratio, a/d, served as the primary test variable amongst the three beams containing shear reinforcement and ranged from 2.5 for the shortest length beam to 5.5 for the longest beam. Regularly spaced 63 mm-long shear studs were provided for beam SP1-5, and 152 mm-length studs were provided for the three shear-reinforced beams. A summary of relevant SC beam details and mechanical properties is provided in Table 3.

One of the finite-element meshes developed for the Varma et al. (2011) SC beams is presented in Fig. 9. Half-span models consisting of eight SC shell elements for the shortest beam (SP2-2), 10 shell elements for the intermediate length beams (SP1-5 and SP2-1) (Fig. 9), and 12 shell elements for the longest beam (SP2-3) were created. In all cases, the longitudinal planar dimensions of the shell elements comprising the shear span regions were typically in the order of 40–50% of the overall beam depths. Overhanging segments of the beams extending beyond the end supports were not included in the finite-element models. The SC shell elements were subdivided into 40 equal thickness concrete layers, and an additional two layers were used to represent the steel faceplates

Table 3. Varma Beam Tests Used for Out-of-Plane Verification

SC beam	Span, L (m)	Width, b (mm)	a/d (mm)	f'_c (MPa)	Aggregate (mm)[a]	$\rho_s = t_p/d$ (%)[b]	ρ_v (%)	$f_{y,\text{plate}}$ (MPa)	$f_{y,\text{ties}}$ (MPa)
SP1-5	5.8	870	3.5	42.7	19	1.43	0	490	—
SP2-1	8.2	860	3.5	48.3	38	2.10	0.15	400	645
SP2-2	8.2	860	2.5	52.4	38	2.10	0.15	426	645
SP2-3	11.3	860	5.5	51.7	38	2.10	0.15	388	645

[a]Nominal maximum coarse aggregate size.
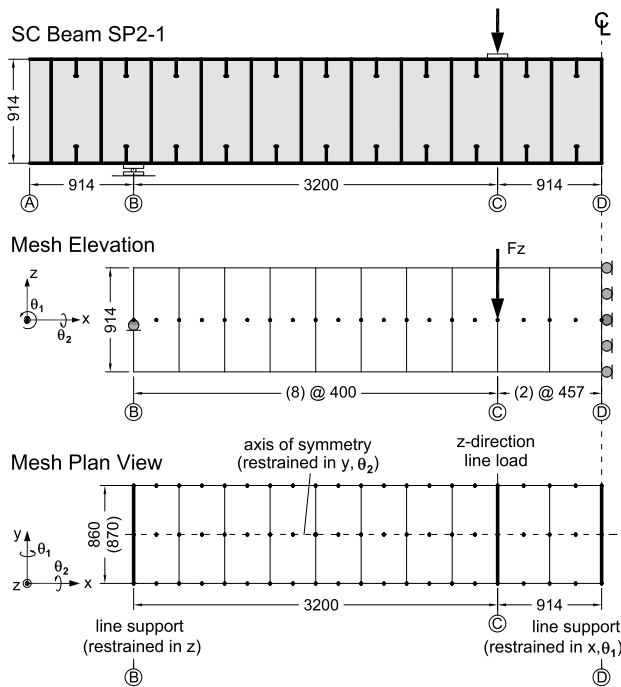[b]Flexural tensile reinforcement ratio.

Fig. 9. Specimen configuration and finite-element modeling; Varma et al. (2011) SC composite beam SP2-1 (half-span shown)

located on the surfaces of the elements. For the SC beams constructed with tie bars, out-of-plane shear reinforcement was smeared throughout the core concrete layers. A line of vertical nodal restraints provided across the widths of the beams represented

the end support reactions, and axial and rotational restraints provided at the midspan locations of the beams were used to enforce symmetry. Loads were applied in a displacement-controlled manner using an increment of 0.50 mm for all beams with the exception of the longest beam, SP2-3, which was analyzed using a displacement increment of 1.00 mm. Member self-weight was insignificant and thus neglected in all cases.

The computed total load-displacement responses for the four SC beams are plotted alongside the experimental results in Fig. 10. For the beams constructed with tie bars [Fig. 10(a)], the layered smeared crack analysis procedure estimated the initial stiffnesses, capacities, and failure modes of the SC beams with reasonable levels of accuracy. In agreement with that reported in the testing program, brittle shear failure modes were estimated to occur in beams SP2-1 ($a/d = 3.5$) and SP2-2 ($a/d = 2.5$), and a ductile flexurally governed failure mode was computed for beam SP2-3 ($a/d = 5.5$). In the analysis of beam SP1-5, which was constructed without tie bar reinforcement, the analysis procedure correctly captured the diagonal tension failure that ultimately controlled the capacity of the beam; however, it provided an out-of-plane shear strength estimate that corresponded to approximately only 75% of the experimental load capacity [Fig. 10(b)]. In prior verification studies, the use of the layered thick-shell element procedure in the analyses of conventional RC members containing no out-of-plane shear reinforcement has shown to provide reliable shear strength estimates for one-way beam-type elements (Hrynyk and Vecchio 2015a). Thus, the conservative assumptions that were used in the development of the SC shell element analysis procedure may, at least in part, be responsible for the reduced capacity estimated for SC beam SP1-5. Specifically, neglecting all tension stiffening effects stemming from the steel faceplates and assuming that the average crack spacing of the SC elements is equal to the full
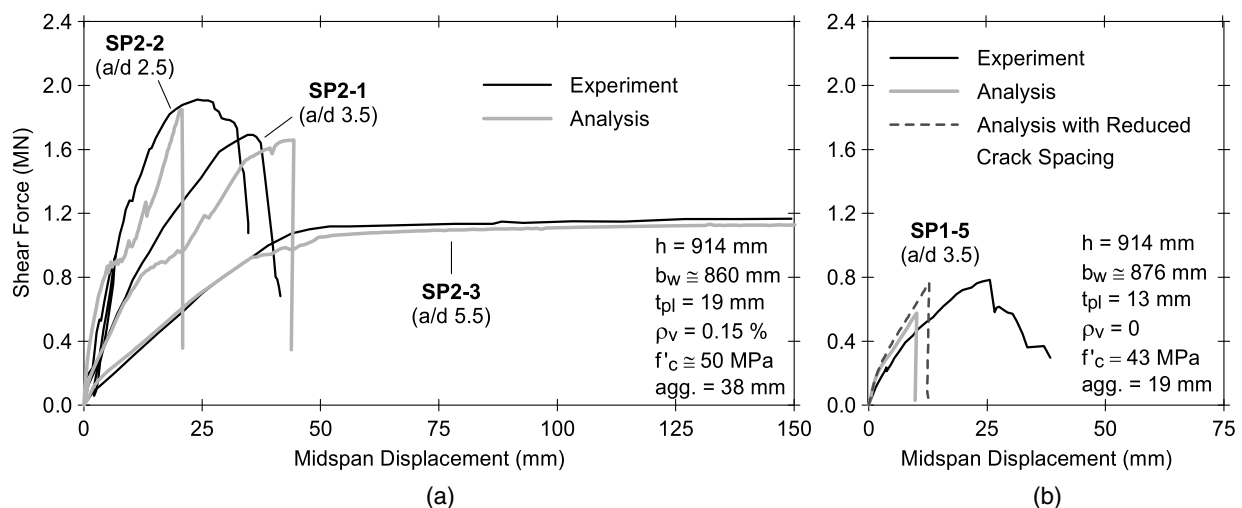

Fig. 10. Computed load-displacement responses for Varma et al. (2011) large-scale SC composite beams: (a) with tie bars; (b) without tie bars

member depth are both likely conservative assumptions. For investigation purposes, the analysis of beam SP1-5 was also performed using a modified maximum average crack spacing value. Reducing the average crack spacing from the full member depth to one-half of the depth (selected arbitrarily for illustration purposes) leads to reduced crack width estimates which, in turn, results in an enhanced aggregate interlock contribution toward element shear resistance. In the case of SC beam SP1-5, the use of the reduced crack spacing provides an estimate of beam shear capacity that is in better agreement with that observed from the testing program. Although there is little data to support a recommendation for generally applicable crack spacing parameters for SC composites, it is clear that the assumptions pertaining to SC element crack spacing are significant and further investigation regarding appropriate SC crack spacing formulations is warranted.

Performance under Combined In-Plane and Out-of-Plane Shear

Relevant to many of the structures that have identified SC composite construction as a potentially viable construction alternative is the need for structural elements that can perform adequately under combined in-plane and out-of-plane loading conditions. Under extreme loading conditions (e.g., seismic ground motions) or in regions comprising atypical geometries (e.g., connection regions), SC composite structures that are designed to function as membranes may experience out-of-plane shear forces in addition to in-plane loads. Thus, using the SC composite shell structure analysis procedure presented in this work, a numerical assessment of the estimated performance of a SC composite wall element under combined in-plane and out-of-plane shear has been performed. For comparative purposes, the geometries and reinforcement levels considered in the assessment have been defined to closely match those comprising a series of conventional RC structural shell elements that have been tested under different combinations of combined in-plane and out-of-plane shear forces (Adebar and Collins 1991). The RC thick-shell analysis procedure forming the basis of the SC composite analyses presented in this work has been previously used to analyze the Adebar and Collins (1991) RC structural shells and was shown to provide reliable estimates for element capacities and accurately captured the governing failure modes observed from testing (Hrynyk and Vecchio 2015a).

The Adebar and Collins (1991) experimental program forming the basis of the numerical investigation consisted of shell-type RC elements that were approximately $1,600 \times 1,600$ mm square and were 310 mm thick. The elements were reinforced with two sets of orthogonal in-plane reinforcement grids that were skewed at an angle of 45° from the edges of the square specimens and had equal reinforcement ratios in the in-plane orthogonal directions. To match the typical geometries and reinforcement ratios provided in the RC shell element tests, the SC composite elements comprising the numerical investigation were assigned identical shell element geometries and equivalent reinforcement levels. The composite elements were reinforced with 5.7 mm-thick steel faceplates, resulting in an in-plane reinforcement ratio of 3.65% and contained a through-thickness tie bar reinforcement ratio of 0.08%. To match the typical material properties comprising the test program elements, the concrete cylindrical compressive strength was taken as 52 MPa with a maximum nominal aggregate size of 20 mm. The uniaxial yield strength of the steel faceplates was taken as 510 MPa, and the yield strength of the tie bar reinforcement was taken as 460 MPa. Two different shear stud densities were considered for the SC composite shells: (1) a b/t
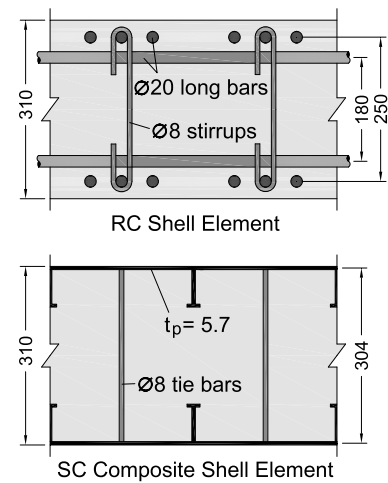

Fig. 11. Shell element cross sections comprising numerical investigation

ratio of 20 which, in accordance with Eq. (2), is adequate in preventing the development of elastic buckling in the 510 MPa faceplates; and (2) a b/t ratio of 30, which is susceptible to faceplate elastic buckling. The through-thickness cross sections of the test-representative RC shell element and the equivalent SC composite element are presented in Fig. 11.

The finite-element mesh used to model the structural shell elements is presented in Fig. 12. This mesh is identical to that previously used in the analyses of the Adebar and Collins (1991) RC shell tests (Hrynyk and Vecchio 2015a). The structural shells were
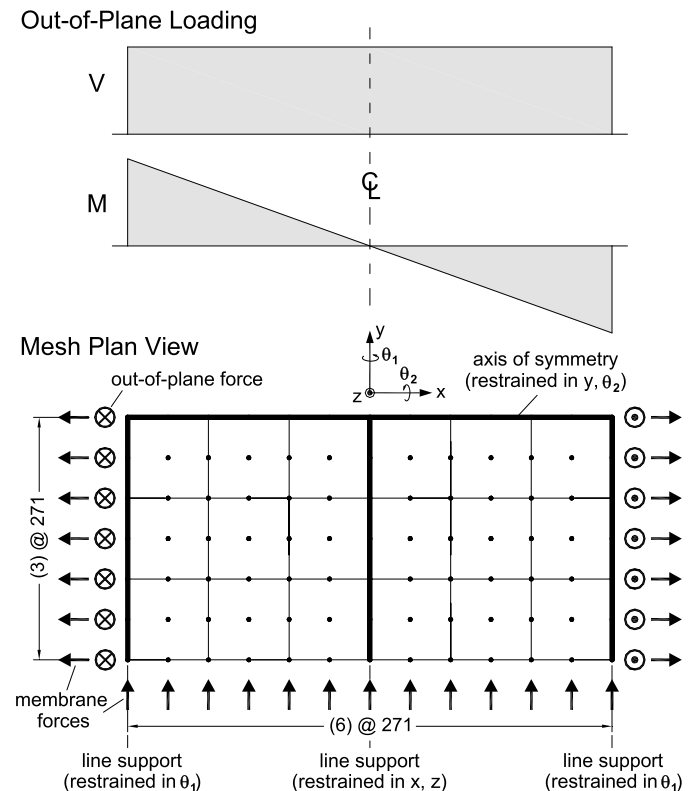

Fig. 12. Loading configuration and finite-element mesh; structural shells (reprinted from Hrynyk and Vecchio 2015a, © ASCE)
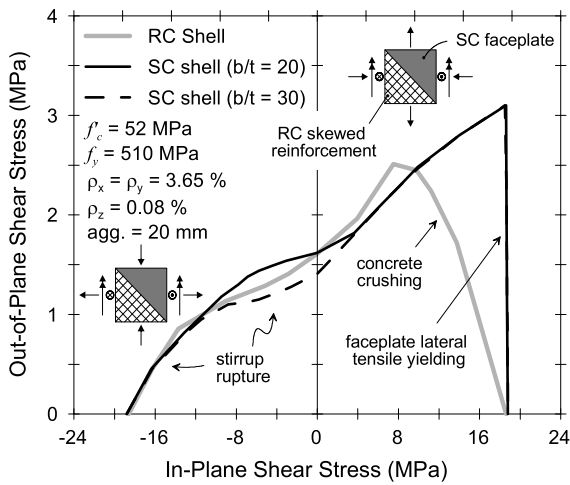
Fig. 13. Computed in-plane to out-of-plane shell element shear strength interaction

analyzed under out-of-plane shear forces and bending moments that were applied about a single axis. Taking advantage of symmetry, only half of the planar surface of the square shell element was considered in the finite-element modeling. The mesh consisted of 18 shell elements that were subdivided into 30 concrete layers. An additional four material layers were used to represent the in-plane steel reinforcing bars comprising the conventional RC elements (two layers for each orthogonal direction), and two additional material layers were used to represent the steel faceplates in the SC composite elements. Through-thickness reinforcement was smeared throughout the concrete material layers; however, conventional RC shell elements did not consider out-of-plane reinforcement in the material layers representing the cover concrete. Similar to the procedure used in the RC shell experimental program, membrane and out-of-plane nodal forces were applied along the perimeters of the shell elements in a manner that produced uniform in-plane shear stress and constant out-of-plane shear force (Fig. 12). Nodal loads were applied in fixed proportions using a load increment equal to approximately 1% of the failure loads reported for the Adebar and Collins (1991) testing program.

The in-plane (i.e., membrane) to out-of-plane shear stress interaction responses computed for the conventional RC and the SC composite structural shell elements are plotted in Fig. 13. Capacity results for SC composite elements utilizing b/t ratios equal to 20 (solid black line) and 30 (dashed line) have been included. Fig. 13 shows that the computed strengths of the RC and the SC composite shell elements under combined in-plane and out-of-plane shear loading were found to be highly sensitive to the orientation of the in-plane stresses acting on the elements. Under negative in-plane shear stress, membrane tensile stresses that contribute to the development and widening of cracks attributed to out-of-plane loading are estimated to reduce the out-of-plane shear capacity; and under positive in-plane shear stress, additive compressive membrane stresses acting along the longitudinal line of action are estimated to increase the out-of-plane shear capacity. In comparing the responses obtained for the RC and the SC composite shell elements, the results from the SC shell element analysis procedure show that the SC element, with reinforcement equivalent to that of the RC element, is estimated to be capable of achieving capacities that are generally comparable or greater than those estimated to cause failure in the RC elements. Under pure membrane shear, steel yielding was estimated to govern element capacity, and

the analysis procedure provided identical strength estimates for the RC and SC composite elements. Under out-of-plane shear loading conditions without the addition of membrane shear, Fig. 13 shows that even with the potentially conservative assumptions made regarding faceplate tension stiffening effects and element crack spacing, the increased effective depth of the SC composite element (Fig. 11) led to out-of-plane shear capacities that were similar to that computed for the conventional RC shell element. In fact, preventing the development of faceplate buckling in the analysis of the SC composite element (i.e., $b/t = 20$) led to SC element capacity estimates that exceeded the capacities of the RC shell elements under isolated out-of-plane loading.

The greatest differences in the capacity estimates obtained for the RC and SC composite shell elements were found to occur under large values of positive membrane shear. In these cases, the RC shell elements were estimated to be governed by crushing of concrete which occurred as a result of the large in-plane compressive stresses acting along the line of action combined with the tensile stresses developed in the skewed in-plane reinforcement. In contrast, under large values of positive membrane shear, the ultimate capacities of the SC composite shell elements were governed by tensile yielding of the steel faceplates in the lateral directions of the elements (i.e., perpendicular to the line of action associated with out-of-plane loading). Because the steel faceplates comprising the SC elements are capable of resisting coexisting axial compressive stresses and lateral tensile stresses, the in-plane compressive resistances of these elements under in-plane shear loading conditions were estimated to be significantly greater than those of the conventional concrete element constructed with steel reinforcing bars that can essentially only carry stresses uniaxially. Thus, the ability of the steel faceplates to resist multiaxial stresses, including planar shear stresses, is a significant feature of the SC composite elements and, on the basis of the proposed analysis procedure, is estimated to provide meaningful performance benefits under certain multiaxial loading conditions. Additionally, even with the use of conservative assumptions regarding faceplate-concrete interaction, the analysis procedure presented suggests that SC composite elements are capable of achieving capacities that are indeed similar to, or greater than, those achievable by conventional RC elements.

Conclusions

A smeared crack nonlinear finite-element analysis procedure for SC composite shells has been presented. Constitutive formulations and assumptions used in the modeling of the characteristic steel faceplates comprising SC element construction were introduced, and their numerical implementation was discussed. The adequacy of the shell structure analysis program was verified using data pertaining to SC composite structures under exclusively in-plane or out-of-plane loading scenarios. Lastly, the analysis procedure was used to provide an assessment of the relative performance of SC composite elements under combined in-plane and out-of-plane loading scenarios. The work presented in this study supports the following conclusions:

1. The finite-element analysis procedure developed on the basis of the constitutive formulations of the disturbed stress field model is a viable approach for the analysis of SC composite infrastructure. The use of the smeared crack formulation within the framework of a layered thick-shell finite element serves as a practical modeling approach permitting reduced computational cost relative to the alternative finely detailed solid element modeling.
2. The SC composite shell structure analysis procedure was shown to provide accurate estimates of strengths and failure modes for

SC members under a broad range of loading conditions. In-plane member behavior was represented well by the membrane performance of the SC composite shell finite elements, and the behaviors of members governed by out-of-plane response mechanisms, including brittle out-of-plane shear failures, were adequately captured using the through-thickness layered formulation of the thick-shell elements employed.

3. The comparative assessment of SC element performance done on the basis of the SC composite analysis procedure developed suggested that even with the use of potentially conservative modeling assumptions, SC composite elements subjected to combined in-plane and out-of-plane shear loading scenarios were estimated to achieve capacities that were similar to or greater than those achieved by conventional RC elements.

Acknowledgments

References

AASHTO. (2014). *LRFD bridge design specifications*, Washington, DC.

Adebar, P. E., and Collins, M. P. (1991). "Shear design of concrete offshore structures." *ACI Struct. J.*, 91(3), 324–335.

Bentz, E. C. (2005). "Explaining the riddle of tension stiffening models for shear panel experiments." *J. Struct. Eng.*, 10.1061/(ASCE)0733-9445 (2005)131:9(1422), 1422–1425.

CEB-FIP (Comité Euro-International du Béton Fédération International de la Précontrainte). (1993). "Design of concrete structures." *CEB-FIP: MC 90*, Thomas Telford, London.

Cook, R. D., Malkus, D. S., and Plesha, M. E. (1989). *Concepts and applications of finite element analysis*, Wiley, New York.

CSA (Canadian Standards Association). (2004). "Design of concrete structures." *CSA A23.3*, Mississauga, ON, Canada.

Dhakal, R. P., and Maekawa, K. (2002a). "Modeling for postyield buckling of reinforcement." *J. Struct. Eng.*, 10.1061/(ASCE)0733-9445(2002) 128:9(1139), 1139–1147.

Dhakal, R. P., and Maekawa, K. (2002b). "Reinforcement stability and fracture of cover concrete in reinforced concrete members." *J. Struct. Eng.*, 10.1061/(ASCE)0733-9445(2002)128:10(1253), 1253–1262.

Epackachi, S., Nguyen, N. H., Kurt, E. G., Whittaker, A. S., and Varma, A. H. (2014). "In-plane seismic behavior of rectangular steel-plate composite wall piers." *J. Struct. Eng.*, 10.1061/(ASCE)ST.1943-541X.0001148, 04014176.

FIB (Fédération Internationale du Béton). (2012). "Model Code 2010, final draft, vol. 1. FIB." *Bulletin 65*, Lausanne, Switzerland.

Figueiras, J. A., and Owen, D. R. J. (1984). "Analysis of elasto-plastic and geometrically nonlinear anisotropic plates and shells." *Finite element software for plates and shells*, E. Hinton and D. R. J. Owen, eds., Pineridge, Swansea, U.K., 403.

Hoshikuma, J., Kawashima, K., Nagaya, K., and Taylor, A. W. (1997). "Stress-strain model for confined reinforced concrete in bridge piers." *J. Struct. Eng.*, 10.1061/(ASCE)0733-9445(1997)123:5(624), 624–633.

Hrynyk, T. D. (2013). "Behaviour and modelling of reinforced concrete slabs and shells under static and dynamic loads." Ph.D. dissertation, Dept. of Civil Engineering, Univ. of Toronto, Toronto.

Hrynyk, T. D., and Vecchio, F. J. (2015a). "Capturing out-of-plane shear failures in the analysis of reinforced concrete shells." *J. Struct. Eng.*, 10 .1061/(ASCE)ST.1943-541X.0001311, 04015058.

Hrynyk, T. D., and Vecchio, F. J. (2015b). "The influence of lateral expansions on the response of steel-concrete composite structures." *23rd Int. Conf. on Structural Mechanics in Reactor Technology (SMiRT-23)*, IASMiRT, Raleigh, NC.

Kupfer, H., Hilsdorf, H. K., and Rusch, H. (1969). "Behavior of concrete under biaxial stress." *ACI J.*, 87(2), 656–666.

Link, R. A., and Elwi, A. E. (1995). "Composite concrete-steel plate walls: Analysis and behavior." *J. Struct. Eng.*, 10.1061/(ASCE)0733-9445 (1995)121:2(260), 260–271.

Malushte, S. R., Booth, P. N., and Varma, A. H. (2009). "Design of modular composite walls subjected to thermal and mechanical loading." *Structures Congress 2009: Don't Mess with Structural Engineers: Expanding Our Role*, ASCE, RestonVA.

Mindlin, R. D. (1951). "Influence of rotary inertia and shear on flexural motions of isotropic, elastic plates." *J. Appl. Mech.*, 18(1), 31–38.

Ozaki, M., Akita, S., Osuga, H., Nakayama, T., and Adachi, N. (2004). "Study on steel plate reinforced concrete panels subjected to cyclic in-plane shear." *Nucl. Eng. Des.*, 228(1–3), 225–244.

Polak, M. A., and Vecchio, F. J. (1993). "Nonlinear analysis of reinforced concrete shells." *J. Struct. Eng.*, 10.1061/(ASCE)0733-9445(1993) 119:12(3439), 3439–3462.

Richart, F. E., Brandtzaeg, A., and Brown, R. L. (1928). "A study of the failure of concrete under combined compressive stresses." *Bulletin 185*, Univ. of Illinois Engineering Experimental Station, Urbana, IL.

Sasaki, N., Akiyiama, H., Narikawa, M., Hara, K., Takeuchi, M., and Usami, S. (1995). "Study on a concrete filled steel structure for nuclear power plants—Part 3: Shear and bending loading tests on wall member." *13th Int. Conf. on Structural Mechanics in Reactor Technology (SMiRT-13)*, IASMiRT, Raleigh, NC.

Seckin, M. (1981). "Hysteretic behaviour of cast-in-place exterior beam-column-slab subassemblies." Ph.D. dissertation, Dept. of Civil Engineering, Univ. of Toronto, Toronto, 266.

Sener, K. C., and Varma, A. H. (2014). "Steel-plate composite walls: Experimental database and design for out-of-plane shear." *J. Constr. Steel Res.*, 100, 197–210.

Takeuchi, M., Narikawa, M., Matsuo, I., Hara, K., and Usami, S. (1998). "Study on a concrete filled structure for nuclear power plants." *Nucl. Eng. Des.*, 179(2), 209–223.

Tanaka, Y., Mochizuki, O., Hirono, T., and Kanou, K. (1998). "Evaluation of steel-concrete composite structures for multi-micro shield tunnel." *Proc., Int. Association for Bridge and Structural Engineering (IABSE) Colloquium: Tunnel Structures*, Vol. 78, Transport Research Laboratory, Berkshire, U.K., 187–192.

Usami, S., Akiyama, H., Narikawa, M., Hara, K., Takeuchi, M., and Sasaki, N. (1995). "Study on a concrete filled steel structure for nuclear power plants—Part 2: Compressive tests on wall members." *13th Int. Conf. on Structural Mechanics in Reactor Technology (SMiRT-13)*, IASMiRT, Raleigh, NC.

Varma, A. H., Sener, K. C., Zhang, K., Coogler, K., and Malushte, S. R. (2011). "Out-of-plane shear behavior of SC composite structures." *21st Int. Conf. on Structural Mechanics in Reactor Technology (SMiRT-21)*, IASMiRT, Raleigh, NC.

Vecchio, F. J. (2000). "Disturbed stress field model for reinforced concrete: Formulation." *J. Struct. Eng.*, 10.1061/(ASCE)0733-9445(2000)126:9 (1070), 1070–1077.

Vecchio, F. J., and Collins, M. P. (1986). "The modified compression field theory for reinforced concrete elements subjected to shear." *ACI J.*, 83(2), 219–321.

Vecchio, F. J., and McQuade, I. (2011). "Towards improved modelling of steel-concrete composite wall elements." *Nucl. Eng. Des.*, 241(8), 2629–2642.

Walraven, J. C., and Reinhardt, H. W. (1981). "Theory and experiments on the mechanical behaviour of cracks in plain and reinforced concrete subjected to shear loading." *Heron*, 26(1), 1–68.

Wong, P., Vecchio, F. J., and Trommels, H. (2013). *VecTor2 and formworks manual*, 2nd Ed., Univ. of Toronto, Toronto, 347.

Zhang, K., Varma, A., Malushte, S. R., and Gallocher, S. (2014). "Effect of shear connectors on local buckling and composite action in steel concrete composite walls." *Nucl. Eng. Des.*, 269, 231–239.

Zhou, J., Mo, Y. L., Sun, X., and Lim, J. (2010). "Seismic performance of composite steel plate reinforced concrete shear wall." *Proc., Conf. on Earth and Space 2010: Engineering, Science, Construction, and Operations in Challenging Environments*, ASCE, Reston, VA, 3002–3010.